

Pre-impulsive and Impulsive Phases of the Sub-Terahertz Flare of March 28, 2022

G.G. MOTORINA,^{1, 2, 3} YU.T. TSAP,⁴ V.V. SMIRNOVA,⁴ A.S. MORGACHEV,¹ A.D. SHRAMKO,¹ AND A.S. MOTORIN⁵

¹*Central Astronomical Observatory at Pulkovo of Russian Academy of Sciences, St. Petersburg, 196140, Russia*

²*Ioffe Institute, Polytekhnicheskaya, 26, St. Petersburg, 194021 Russia*

³*Astronomical Institute of the Czech Academy of Sciences, 251 65 Ondřejov, Czech Republic*

⁴*Crimean Astrophysical Observatory, Russian Academy of Sciences, Nauchnyi, Russia*

⁵*ITMO University, 197101 St. Petersburg, Russia*

(Received February 27, 2023)

Abstract

Properties of the solar radio spectrum, as well as the temporal profiles of flare emission, indicate the thermal nature of the sub-terahertz (sub-THz) component observed as the growth of radio emission in the frequency range of 100–1000 GHz. The sub-THz flare onset can be ahead of the impulsive phase for several minutes. However, the origin of the pre-impulsive and impulsive sub-THz emission remains unclear. The present work is devoted to a detailed analysis of the M4.0 X-class solar flare observed on March 28, 2022 with the Bauman Moscow State Technical University Radio Telescope RT-7.5 at 93 GHz. We supply these data with multiwavelength solar observations in the X-ray (GOES, GBM/Fermi), extreme ultraviolet (AIA/SDO), and microwave ranges. The differential emission measure (DEM) responsible for EUV emission is determined by solving the inverse problem based on the AIA/SDO data. Using the DEM and assuming a thermal free-free emission mechanism in pre-impulsive and impulsive phases, we calculated the millimeter emission flux of coronal plasma of the flare source, which turned out to be much smaller than the observed values. We concluded that electrons accelerated in the corona and heat fluxes from the coronal loop top cannot be responsible for heating the sub-THz emission source located in the transition region and upper chromosphere. A possible origin of chromospheric heating in the pre-impulsive phase of the solar flare is discussed.

Keywords: Sun: Flares - Sun: X-rays, EUV, Radio emission

1. INTRODUCTION

Relatively recently, it became possible to carry out regular solar observations in the sub-terahertz (sub-THz) range of the electromagnetic spectrum at frequencies of 100–1000 GHz (Kaufmann et al. 2001; Krucker et al. 2013). This has opened a new window of opportunity to study the nature of solar flares. In particular, the unusual increase in sub-THz flux between 212 and 405 GHz during the solar flare on March 22, 2000 (Kaufmann et al. 2001), the mechanism of which is still highly controversial (Krucker et al. 2013; Kontar et al. 2018; Tsap et al. 2018), marked the emergence of a new direction in solar radio astronomy research.

Modern Atacama Large Millimeter Array (ALMA) observations of the Sun (Wedemeyer et al. 2016; Alissandrakis et al. 2017) have allowed to obtain the structure of the upper layers of the solar atmosphere in the previously inaccessible sub-THz range. As of today, only six weak solar flares have been registered with ALMA, one event

(Shimizu et al. 2021) in the interferometric mode at 100 GHz and five flares (Skokić et al. 2023) at 100 GHz ($\lambda = 3$ mm) or 240 GHz ($\lambda = 1.2$ mm) in the single-dish scanning mode, as necessary for image calibration. It has been shown (see, e.g., Alissandrakis et al. (2017)) that images of the transition region and upper chromosphere observed in the sub-THz and ultraviolet (1600 Å) ranges exhibit similar magnetic structures. In contrast, based on observations at 1.2 and 3 mm with spatial resolutions of about 28'' and 60'' respectively, Skokić et al. (2023) identified sources of millimeter radiation with hot loops visible in SDO/AIA. However, the temporal resolution of these observations was low, approximately ~ 5 (3 mm) and ~ 10 (1.2 mm) minutes, making the conclusions of Skokić et al. (2023) less convincing.

The problem of flare atmospheric heating and energy transfer of accelerated particles to the dense layers of the chromosphere/photosphere remains unresolved. In particular, X-ray sources in the preimpulsive phase of a flare

may be located at the footpoints of coronal loops, and their temperatures may reach 10-15 MK (Hudson et al. 2021). On the other hand, sub-THz emission is associated with X-ray emission (Kaufmann et al. 2009), for the generation of which the thermal plasma of the corona, transition region, and upper chromosphere may be responsible. This suggests that the study of the sub-THz and X-ray sources can give valuable information about the heating of the chromospheric plasma, which can be caused by accelerated electrons, thermal fluxes, shock waves, as well as *in situ* flare energy release.

The aim of this study is to investigate the role of coronal thermal plasma and accelerated electrons in generating the sub-THz radiation based on the SOL2022-03-28T105800 flare event, as well as to try to understand the nature of heating in the transition region and upper chromosphere of the Sun, primarily in the pre-impulsive phase of the solar flare.

2. OBSERVATIONAL DATA AND PROCESSING

The SOL2022-03-28T105800 solar flare was selected for the analysis of the heating source in the preimpulsive phase, since it was recorded by the RT-7.5 radio telescope of the Bauman Moscow State Technical University (93 GHz) and was observed by several other instruments across a wide wavelength range. The SOL2022-03-28T105800 flare of X-ray class M4.0 occurred in active region NOAA 12975 between 10:58 and 11:45 UT, with the maximum of sub-THz emission at 11:28 UT.

To accomplish the task, the extreme ultraviolet (EUV) data at 94, 131, 171, 193, 211, and 335 Å wavelengths were analyzed. These data were obtained using the Atmospheric Imaging Assembly on board Solar Dynamic Observatory (AIA/SDO) (Lemen et al. 2012). The X-ray radiation data from the Fermi Gamma-ray Burst Monitor (GBM/Fermi) (Meegan et al. 2009) and the Geostationary Operational Environmental Satellite (GOES) (White et al. 2005) were also employed (Figs.1a, 1b). These instruments provide information about the thermal flare plasma and nonthermal accelerated electrons. Furthermore, for a more detailed analysis of the SOL2022-03-28T105800 flare the data from the Kislovodsk Mountain Astronomical Station obtained with RT-2 and RT-3 radio telescopes at frequencies of 6 and 9 GHz, respectively (<http://solarstation.ru/>, Shramko (2004)), the RT-7.5 radio telescope of Bauman Moscow State Technical University (93 GHz, Rozanov (1981); Smirnova et al. (2016)) (Figs.1c, 1d), Metsähovi Radio Observatory (11.2 GHz, Kallunki et al. (2018)), and the observatory of the Italian National Institute for Astrophysics (INAF, 26 GHz, Pellizzoni et al. (2022)) were included.

The time profile of sub-THz radiation at 93 GHz (Fig.1d) was constructed from the maps (Fig.1e) obtained with the RT-7.5 radio telescope. In each map, the active region in which the flare occurred was identified, followed by the calculation of the maximum flux value. It is evident from Fig.1d that during the pre-impulsive phase of the flare from 11:00:00 to 11:00:12 UT, the spectral flux density of sub-THz radiation increases, reaching approximately 20 sfu. The procedures for calibrating the sub-THz radiation flux at the RT-7.5 radio telescope, including noise estimates of the receiving equipment, atmospheric absorption coefficients, tracking error uncertainties, etc., align with those described by Tsap et al. (2016) and Ryzhov et al. (2016). Thus, we used standard observational calibration methods utilized in sub-THz (millimeter) radio astronomy (Kaufmann et al. 2001).

What draws attention first of all is the similarity of the time profiles of microwave and hard X-ray emission (Figs.1a, 1c), which consisted of multiple peaks. Although observations in the sub-THz range were carried out only at 93 GHz, the spectral flux density spectrum of the SOL2022-03-28T105800 solar flare (Fig.1f) indicates that it was positive between frequencies of 26 and 93 GHz, with a power-law index $\alpha \approx 0.6$. The error estimates are indicated on the spectrum by bars in Fig.1f.

Using the AIA/SDO data (Fig.2) at two time intervals corresponding to the beginning of the flare (11:00:00–11:00:12 UT) and the peak of the impulsive phase (11:28:00–11:28:12 UT) of the millimeter burst, we performed the reconstruction of the differential emission measure (DEM, Fig.3) using the regularization technique (Tikhonov & Arsenin 1979; Hannah & Kontar 2012):

$$\phi(T) = n_e^2 \frac{dl}{dT}, \quad (1)$$

where n_e is the electron number density and l is the source size along the line of sight for flare plasma temperatures in the range of $T = 0.5 - 32$ MK.

Based on the obtained distributions $\phi(T)$, calculations were performed for the millimeter emission using the integral brightness temperature T_b and the observed spectral flux F_ν in the assumption of thermal bremsstrahlung emission according to formulas (Dulk 1985; Tsap et al. 2016):

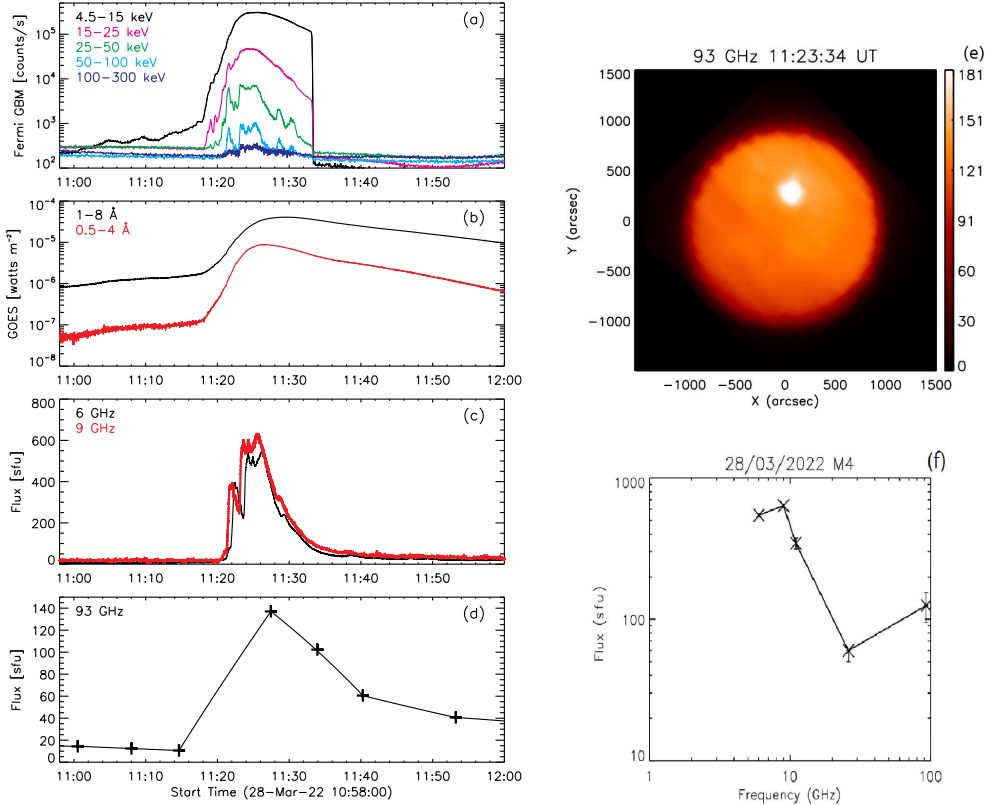


Figure 1. Left: the time profiles of the SOL2022-03-28T105800 solar flare in the X-ray (a, b), microwave (c), and sub-THz (d) ranges. Right: the flare map at 93 GHz (e), the flare flux density spectrum (f).

3. SOURCE OF CHROMOSPHERIC PLASMA HEATING

$$T_b(\nu) = \frac{1}{\nu^2} \int_{T_{\min}}^{T_{\max}} \frac{K\phi(T)}{\sqrt{T}} e^{-\tau_\nu(T)} dT, \quad (2)$$

$$\tau_\nu = \int_{T_{\min}}^{T_{\max}} \frac{K\phi(T)}{T^{3/2}\nu^2} dT, \quad (3)$$

$$F_\nu = \frac{2k_B\nu^2}{c^2} T_b(\nu) \frac{S}{R^2}, \quad (4)$$

in which the standard notation is used.

As follows from Eqs. (2-4), even for the maximum thermal source areas $S = 7.8 \times 10^{18} \text{ cm}^{-3}$, corresponding to the 50% level of the maximum intensity in the EUV maps (Fig.2), the calculated fluxes F_ν at 93 GHz were 1.5 sfu (11:00 UT) and 45 sfu (11:28 UT), respectively. These values were noticeably underestimated compared to the observed values of 20 ± 5 sfu and 125 ± 31 sfu, respectively. Taking into account that filaments in the energy release region were not visible and the contribution of optically thin flare plasma with temperatures $T = 0.5 - 32$ MK to millimeter emission was negligibly small, as indicated by our estimates, we can conclude that the sub-THz component was most likely generated by cool chromospheric plasma.

To estimate the contribution of accelerated electrons to the observed sub-THz emission of the SOL2022-03-28T105800 solar flare, we performed the fitting of the X-ray spectrum using data from the GBM/Fermi satellite, assuming a homogeneous isothermal plasma and a thick-target model. In the initial phase of the flare, 11:00:00–11:00:12 UT, the X-ray emission was comparable to the background values, so the fitting of the GBM/Fermi data was done assuming a homogeneous isothermal plasma excluding the contribution of nonthermal component (Fig.4, left). However, during the period from 11:28:00 to 11:28:12 UT, which corresponded to the peak of the sub-THz emission (Fig.4, right), we also considered the nonthermal component.

This allowed us to estimate within the thick-target model the spectral index of nonthermal accelerated electrons $\delta = 7.86$, the low-energy cutoff $E_0 = 18.57$ [keV], and the total integrated electron flux $F = 8.57 \times 10^{35} \text{ [s}^{-1}\text{]}$. As indicated by the obtained results, the temperature of the X-ray plasma in the pre-impulsive phase of the flare reached $T = 15.37$ MK at negligible value of emission measure $EM = 10^{45} \text{ cm}^{-3}$, which is in a good

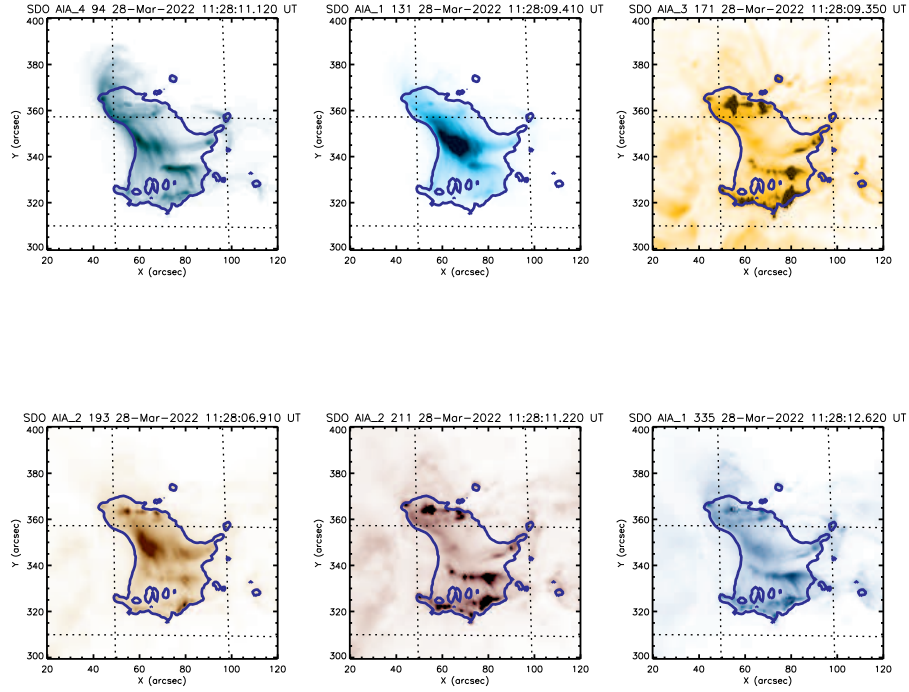


Figure 2. The EUV images of the SOL2022-03-28T105800 solar flare obtained at 94, 131, 171, 193, 211, and 335 Å AIA/SDO passbands. The blue line marks the 50% contour of the intensity maximum.

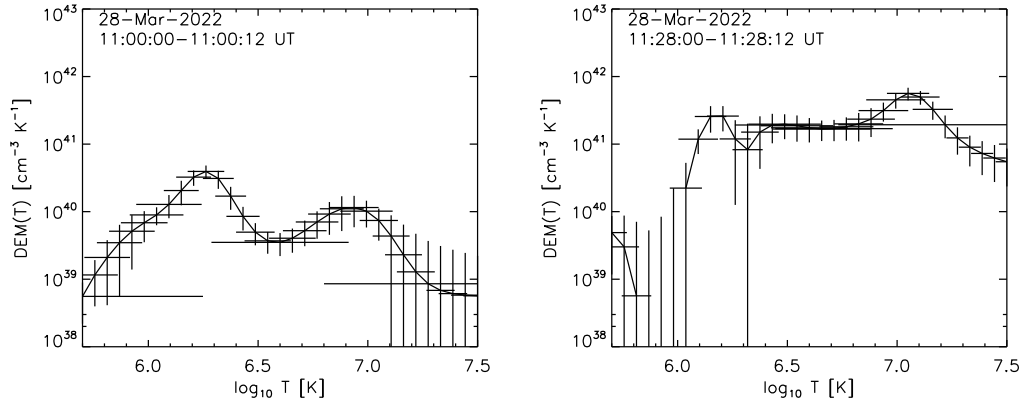


Figure 3. The differential emission measure of the SOL2022-03-28T105800 solar flare estimated for the times 11:00:00–11:00:12 UT (left) and 11:28:00–11:28:12 UT (right).

agreement with the findings of [Hudson et al. \(2021\)](#). Meanwhile, during the peak, $EM = 3.89 \times 10^{49} \text{ cm}^{-3}$ and $T = 17.05 \text{ MK}$, the spectrum of accelerated electrons occurred to be too soft ($\delta = 7.86$) to effectively heat the plasma of the transition region and chromosphere ([Tsap 2008](#); [Morgachev et al. 2021](#)).

Considering the relatively high values of the X-ray plasma temperature both in the pre-impulsive phase

and the flare peak, it might seem that coronal thermal fluxes could be responsible for heating the chromospheric plasma. Let us make some simple estimates.

The rate of heating of the transition region and upper chromosphere plasma due to electron thermal conductivity can be estimated as follows:

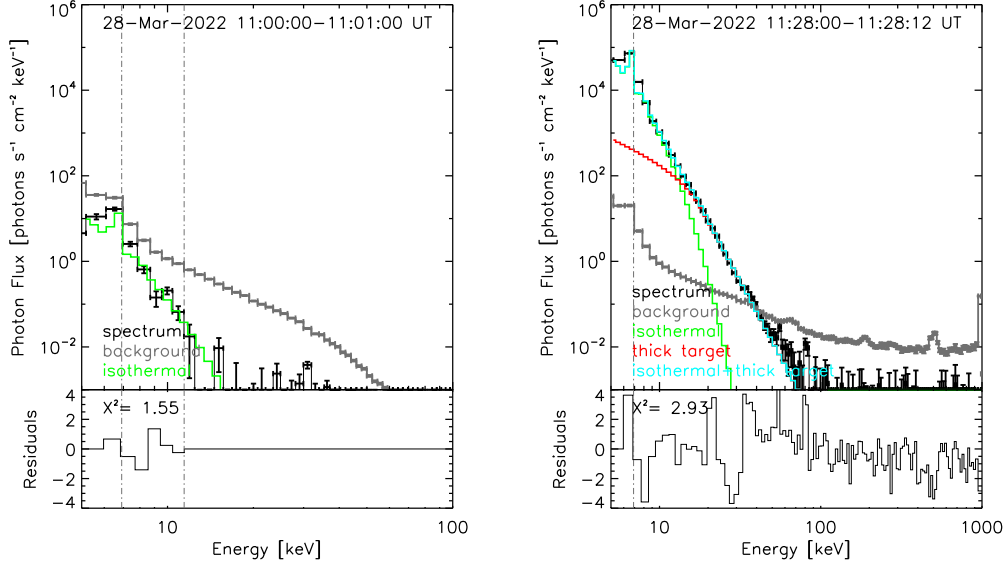


Figure 4. The averaged GBM/Fermi X-ray spectrum (background subtracted data, black line) fitted by the homogeneous isothermal plasma (green line) for the time 11:00:00–11:01:12 UT (right); the homogeneous isothermal plasma (green line) and thick target model (red line) for 11:28:00–11:28:12 UT (left). The summed fit of the spectrum is shown by the blue line. The background is shown by the gray line. The residuals are shown in the bottom panels.

$$q = \kappa \frac{d}{ds} (T^{5/2} \frac{dT}{ds}) = \kappa \frac{2}{7} \frac{d}{ds} (\frac{dT^{7/2}}{ds}) = \kappa \frac{2}{7} \frac{d^2 T^{7/2}}{ds^2} \approx \kappa \frac{2}{7} \frac{T^{7/2}}{s^2} \quad (5)$$

where the electron thermal conductivity coefficient $\kappa = 10^{-6} \text{ erg K}^{-7/2} \text{ s}^{-1}$. Then, assuming thermal energy $W_{\text{th}} = 3/2nkT$, where $k = 1.38 \times 10^{-16} \text{ [erg K}^{-1}]$ is the Boltzmann constant, plasma density $n = 10^{11} \text{ [cm}^{-3}]$, the temperature $T = 10^5 \text{ [K]}$, and plasma layer thickness $s = 3 \times 10^7 \text{ [cm]}$, we obtain the characteristic heating time of the transition region:

$$\tau_{\text{con}} = \frac{W_{\text{th}}}{q} = 21 \frac{kn s^2}{\kappa T^{5/2}} \approx 10^5 \text{ s}. \quad (6)$$

The obtained estimate (~ 28 hours) excludes the possibility of effective heating of not only the chromosphere but also the transition region by coronal thermal fluxes during the flare energy release.

As for shock waves, their significant contribution to chromospheric heating appears doubtful, especially since we did not find any indications of explosive energy release in the pre-impulsive phase.

4. DISCUSSION OF RESULTS AND CONCLUSIONS

In this study, we performed an analysis of the sub-THz, microwave, EUV, and X-ray emission of the SOL2022-03-28T105800 solar flare. This allowed us to determine the contribution of the coronal flare plasma

and accelerated electrons to the generation of sub-THz emission in the pre-impulsive and impulsive (close to the maximum of the flare) phases. It has been shown that the coronal plasma contributes insignificantly to the observed millimeter flare emission at 93 GHz. The parameters of nonthermal electrons, namely, the soft power-law spectrum and the absence of the observable hard X-ray and microwave emission during the initial flare phase indicate the minor contribution of accelerated electrons to chromospheric plasma heating.

The calculated sub-THz fluxes are an order of magnitude smaller than the observed values. This suggests that the contribution of the thermal flare coronal plasma to the sub-THz component is negligibly small. Hence, the conclusion about the important role of an additional energy release source located directly in the solar chromosphere can be drawn. We believe that there was *in situ* heating of the flare chromosphere occurred due to the Joule dissipation of electric current. One of the possible mechanisms based on the interaction of ions with neutral atoms in nonstationary conditions is described in (Stepanov & Zaitsev 2016). Further more detailed investigations require multi-frequency sub-THz observations with high spatial and temporal resolution, since it cannot be fully excluded that heating mechanisms of nonthermal nature also played an important role in the considered case.

ACKNOWLEDGMENTS

The study was in part supported by the State Assignment no. 0040-2019-0025 (G.G. Motorina), Russian Science Foundation grant no. 22-12-00308 (Yu.T. Tsap,

A.S. Morgachev), the Russian Foundation for Basic Research grant no. 20-52-26006 (V.V. Smirnova), Ministry of Education and Science (NIR No. 1021051101548-7-1.3.8; 075-03- 2022-119/1) (A.D. Shramko).

REFERENCES

- Alissandrakis, C. E., Patsourakos, S., Nindos, A., & Bastian, T. S. 2017, *A&A*, 605, A78
- Dulk, G. A. 1985, *ARA&A*, 23, 169
- Hannah, I. G. & Kontar, E. P. 2012, *A&A*, 539, A146
- Hudson, H. S., Simões, P. J. A., Fletcher, L., Hayes, L. A., & Hannah, I. G. 2021, *MNRAS*, 501, 1273
- Kallunki, J., Tornikoski, M., Tammi, J., Kinnunen, E., Korhonen, K., Kesäläinen, S., & Arkko, O. 2018, *Astronomische Nachrichten*, 339, 204
- Kaufmann, P., Giménez de Castro, C. G., Correia, E., Costa, J. E. R., Raulin, J.-P., & Válio, A. S. 2009, *ApJ*, 697, 420
- Kaufmann, P., Raulin, J. P., Correia, E., Costa, J. E. R., de Castro, C. G. G., Silva, A. V. R., Levato, H., Rovira, M., Mandrini, C., Fernández-Borda, R., & Bauer, O. H. 2001, *ApJL*, 548, L95
- Kontar, E. P., Motorina, G. G., Jeffrey, N. L. S., Tsap, Y. T., Fleishman, G. D., & Stepanov, A. V. 2018, *A&A*, 620, A95
- Krucker, S., Giménez de Castro, C. G., Hudson, H. S., Trotter, G., Bastian, T. S., Hales, A. S., Kašparová, J., Klein, K. L., Kretschmar, M., Lüthi, T., Mackinnon, A., Pohjolainen, S., & White, S. M. 2013, *A&A Rv*, 21, 58
- Lemen, J. R., Title, A. M., Akin, D. J., Boerner, P. F., Chou, C., Drake, J. F., Duncan, D. W., Edwards, C. G., Friedlaender, F. M., Heyman, G. F., Hurlburt, N. E., Katz, N. L., Kushner, G. D., Levay, M., Lindgren, R. W., Mathur, D. P., McFeaters, E. L., Mitchell, S., Rehse, R. A., Schrijver, C. J., Springer, L. A., Stern, R. A., Tarbell, T. D., Wuelsel, J.-P., Wolfson, C. J., Yanari, C., Bookbinder, J. A., Cheimets, P. N., Caldwell, D., Deluca, E. E., Gates, R., Golub, L., Park, S., Podgorski, W. A., Bush, R. I., Scherrer, P. H., Gumm, M. A., Smith, P., Aufer, G., Jerram, P., Pool, P., Soufli, R., Windt, D. L., Beardsley, S., Clapp, M., Lang, J., & Waltham, N. 2012, *SoPh*, 275, 17
- Meegan, C., Lichti, G., Bhat, P. N., Bissaldi, E., Briggs, M. S., Connaughton, V., Diehl, R., Fishman, G., Greiner, J., Hoover, A. S., van der Horst, A. J., von Kienlin, A., Kippen, R. M., Kouveliotou, C., McBreen, S., Paciasas, W. S., Preece, R., Steinle, H., Wallace, M. S., Wilson, R. B., & Wilson-Hodge, C. 2009, *ApJ*, 702, 791
- Morgachev, A. S., Tsap, Y. T., Motorina, G. G., Smirnova, V. V., & Motorin, A. S. 2021, *Geomagnetism and Aeronomy*, 61, 1045
- Pellizzoni, A., Righini, S., Iacolina, M. N., Marongiu, M., Mulas, S., Murtas, G., Valente, G., Egron, E., Bachetti, M., Buffa, F., Concu, R., Deiana, G. L., Guglielmino, S. L., Ladu, A., Loru, S., Maccaferri, A., Marongiu, P., Melis, A., Navarrini, A., Orfei, A., Ortu, P., Pili, M., Pisanu, T., Pupillo, G., Saba, A., Schirru, L., Serra, G., Tiburzi, C., Zanichelli, A., Zucca, P., & Messerotti, M. 2022, *SoPh*, 297, 86
- Rožanov, B. A. 1981, *Izvestiia Vysshiaia Uchebn. Zaved., Radiofizika*, 24, 3
- Ryzhov, V., Dimiev, D., & Zharkova, N. 2016, *Radioopt. MGTU im. N.E. Baumana*, 14–23
- Shimizu, T., Shimojo, M., & Abe, M. 2021, *ApJ*, 922, 113
- Shramko, A. 2004, *Izv. Gl. Astron. Obs.*, 555–560
- Skokić, I., Benz, A. O., Brajša, R., Sudar, D., Matković, F., & Bárta, M. 2023, *A&A*, 669, A156
- Smirnova, V., Tsap, Y., Shumov, A., & et al. 2016, *Nauka Obraz.: MGTU im. N. E. Baumana*, 12, 85–97
- Stepanov, A. V. & Zaitsev, V. V. 2016, *Geomagnetism and Aeronomy*, 56, 952
- Tikhonov, A. N. & Arsenin, V. Y. 1979, Moscow: Nauka
- Tsap, Y. 2008, *Doctoral (Phys.–Math.) Dissertation*, St. Petersburg, 14–23
- Tsap, Y. T., Smirnova, V. V., Morgachev, A. S., Motorina, G. G., Kontar, E. P., Nagnibeda, V. G., & Strelakova, P. V. 2016, *Advances in Space Research*, 57, 1449
- Tsap, Y. T., Smirnova, V. V., Motorina, G. G., Morgachev, A. S., Kuznetsov, S. A., Nagnibeda, V. G., & Ryzhov, V. S. 2018, *SoPh*, 293, 50
- Wedemeyer, S., Bastian, T., Brajša, R., Hudson, H., Fleishman, G., Loukitcheva, M., Fleck, B., Kontar, E. P., De Pontieu, B., Yagoubov, P., Tiwari, S. K., Soler, R., Black, J. H., Antolin, P., Scullion, E., Gunár, S., Labrosse, N., Ludwig, H. G., Benz, A. O., White, S. M., Hauschildt, P., Doyle, J. G., Nakariakov, V. M., Ayres, T., Heinzl, P., Karlicky, M., Van Doorselaere, T., Gary, D., Alissandrakis, C. E., Nindos, A., Solanki, S. K., Rouppe van der Voort, L., Shimojo, M., Kato, Y., Zaqarashvili, T., Perez, E., Selhorst, C. L., & Bárta, M. 2016, *SSRv*, 200, 1

White, S. M., Thomas, R. J., & Schwartz, R. A. 2005,
SoPh, 227, 231